LBNL-2001061

Lawrence Berkeley National Laboratory

Security-Constrained Design of Isolated Multi-Energy Microgrids

S. Mashayekh[1], M. Stadler1 G. Cardoso[1], M. Heleno[1], S. Chalil Madathil[2], H. Nagarajan[3], R. Bent[3], M. Mueller-Stoffels[4], X. Lu[5], J. Wang[5]

[1]Lawrence Berkeley National Lab
[2]Department of Industrial Engineering, Clemson University
[3]Center for Nonlinear Studies, Los Alamos National Laboratory
[4]University of Alaska Fairbanks
[5]Argonne National Laboratory

Published in IEEE Transactions on Power Systems

May, 2018

DER-CAM has been funded partly by the Office of Electricity Delivery and Energy Reliability, Distributed Energy Program of the U.S. Department of Energy under Contract No. DE-AC02-05CH11231.

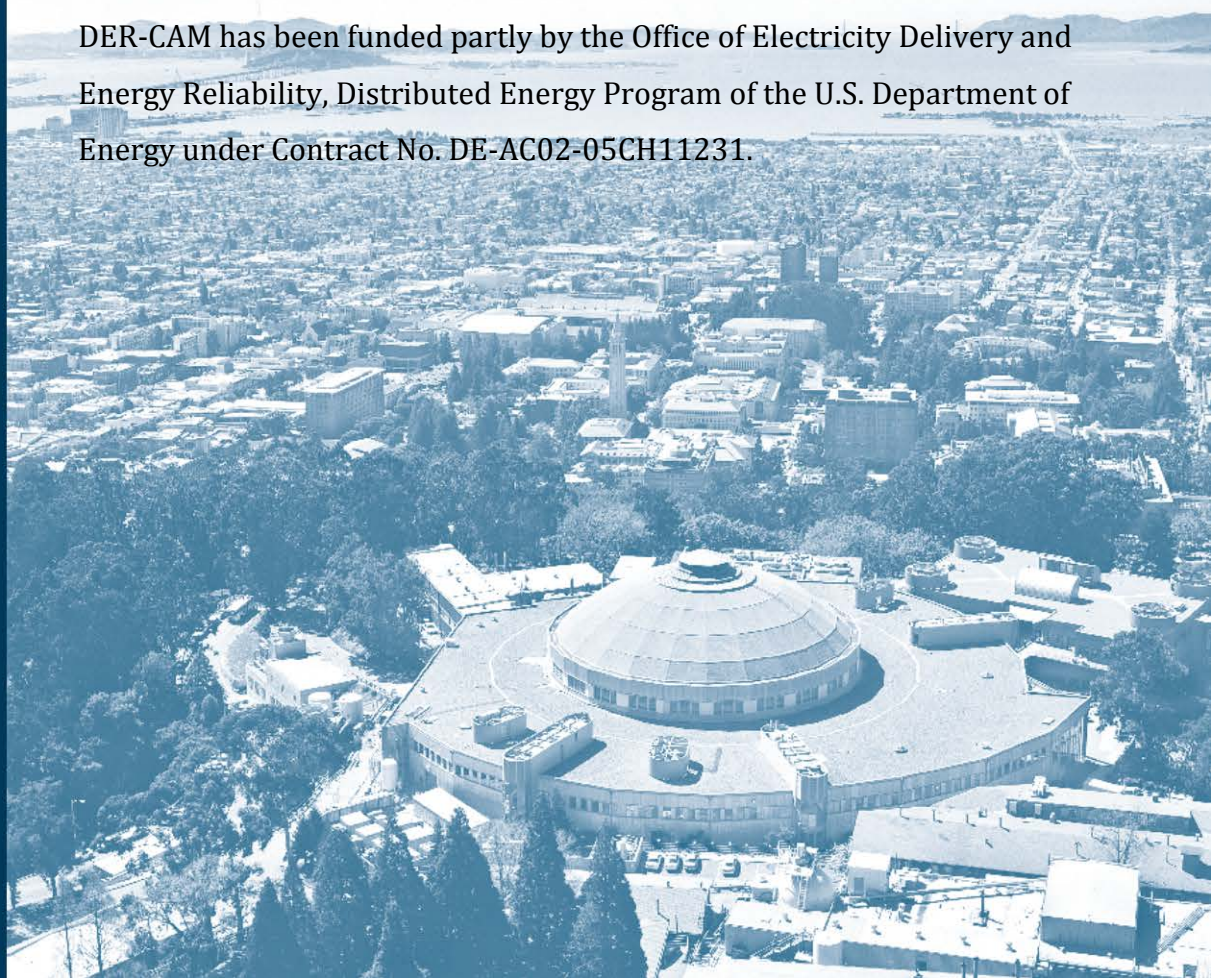

Disclaimer

This document was prepared as an account of work sponsored by the United States Government. While this document is believed to contain correct information, neither the United States Government nor any agency thereof, nor The Regents of the University of California, nor any of their employees, makes any warranty, express or implied, or assumes any legal responsibility for the accuracy, completeness, or usefulness of any information, apparatus, product, or process disclosed, or represents that its use would not infringe privately owned rights. Reference herein to any specific commercial product, process, or service by its trade name, trademark, manufacturer, or otherwise, does not necessarily constitute or imply its endorsement, recommendation, or favoring by the United States Government or any agency thereof, or The Regents of the University of California. The views and opinions of authors expressed herein do not necessarily state or reflect those of the United States Government or any agency thereof or The Regents of the University of California.

Security-Constrained Design of Isolated Multi-Energy Microgrids

Salman Mashayekh[1], *Member, IEEE*, Michael Stadler[1], *Member, IEEE*, Gonçalo Cardoso[1], Miguel Heleno[1], Sreenath Chalil Madathil[2], Harsha Nagarajan[3], Russel Bent[3], Marc Mueller-Stoffels[4], Xiaonan Lu[5], Jianhui Wang[5]

***Abstract*— Energy supply in rural and off-grid communities has traditionally relied on diesel-based microgrids, due to limited access. But global environmental concerns are pushing for the transformation of these systems into renewable-based microgrids. This transition to more complex systems with a mix of dispatchable and non-dispatchable resources requires new planning tools that ensure the security of supply. This paper presents a novel mixed-integer linear optimization model that determines optimal technology mix, size, placement, and associated dispatch for a multi-energy microgrid. The model satisfies microgrid's electrical and heat transfer network limitations by integrating linear power flow and heat transfer equations. It captures the efficiency gains from waste heat recovery through combined heat and power technologies, by modeling the interplay between electrical and heat sources. To ensure a secure design against generator outages, the optimization maintains sufficient reserve capacity in the system, which is dynamically allocated based on system operating conditions. Several case studies on an isolated microgrid model, developed based on a real microgrid in Alaska, illustrate how the proposed model works. The results show the effectiveness of the model and are used to discuss various aspects of the optimization solution.**

***Index Terms*—microgrid, isolated, remote, N-1 contingency, security-constrained, optimal planning, optimal dispatch, mixed integer linear program, MILP**

I. Nomenclature

We denote variables in *italic* fonts, parameters in non-italic fonts, and binary/integer variables with all-small letters. The nomenclature is sorted alphabetically.

Sets and indices

c	continuous generation technologies: photovoltaic (PV), solar thermal (ST), electric chiller (EC), boiler (BL), absorption chiller (AC)
e	edge index for line ampacity constraint approximation
g	discrete generation technologies: internal combustion engine (ICE), micro-turbine (MT), fuel cell (FC) – these technologies may be CHP-enabled.
i	all generation and storage technologies (g ∪ c ∪ s)
j	all generation technologies (g ∪ c)
k	al continuous technologies (c ∪ s)
n, n′	microgrid nodes: 1, 2,…, N
s	storage technologies: electric storage (ES), heat storage (HS), cold storage (CS)
t	time
u	energy use: electricity (EL), cooling (CL), heating (HT)

Parameters

α_j	useful heat recovered from a unit of generated electricity
$\gamma_{n,n'}$	heat loss coefficient for heat transfer pipe (n,n′), % per meter
η_j	electrical efficiency of generation technology j
η_s^C	charging efficiency of storage technology s
η_s^D	discharging efficiency of storage technology s
φ_s	losses due to self-discharge in storage technology s, % per Δt
ϕ	generation or load power factor
Δt	optimization time-step, hour
Δt^{ctg}	post-contingency dispatch period duration, seconds
Δt^{ctgrmp}	post-contingency ramp-up period duration, seconds
AR_i	annuity rate for technology i
CC_n	Curtailment cost (post-contingency) for electrical loads at node n, $/kW
CER_j	carbon emissions rate from generation technology j, kg/kWh
CP^a	coefficient of performance for absorption chiller
CP^e	coefficient of performance for electric chiller
$\overline{CR}_s$	maximum charge rate of storage technology s, % of capacity
$\overline{DR}_s$	maximum discharge rate of storage technology s, % of capacity
$\underline{E}_s$	minimum acceptable energy (state of charge) for storage technology s, %
$\overline{E}_s$	maximum acceptable energy (state of charge) for storage technology s, %
FCC_k	fixed capital cost of continuous technology k, $
GC_j	generation cost (e.g. fuel consumption) of technology j, $/kWh
$\overline{H}_{n,n'}$	heat transfer capacity for pipe (n,n′), kW
M	an arbitrary large number

Corresponding author: Salman Mashayekh (email: smashayekh@lbl.gov). Authors are with [1]Lawrence Berkeley National Laboratory, 1 Cyclotron Road, Berkeley, CA 94720, [2]Department of Industrial Engineering, Clemson University, Clemson, SC 29634 USA, [3]Center for Nonlinear Studies, Los Alamos National Laboratory, Los Alamos, NM, [4]University of Alaska Fairbanks, Fairbanks, AK 99775, and [5]Argonne National Laboratory, Argonne, IL 60439.

N number of electrical/thermal nodes
$\overline{Pg}_g$ maximum operating power of discrete generation technology g, kW
$\underline{Pg}_g$ minimum operating power of discrete generation technology g, kW
$\overline{PgR}_g$ maximum rate of generation increase for discrete technology g, % of capacity
$Pl_{n,u,t}$ load (active load for electricity end-use) for end-use u at node n, kW
$Ql_{n,t}$ reactive electricity load at node n, kVAr
$R_{n,n'}$ resistance of line (n,n′), pu
$\overline{S}_{n,n'}$ power carrying capacity of line (n,n′), pu
Sb microgrid base apparent power, kVA
SP_t solar potential at time t, % of peak capacity
TCC_g turnkey capital cost of discrete generation technology g, $/kW
$\underline{V}$ minimum acceptable voltage magnitude, pu
$\overline{V}$ maximum acceptable voltage magnitude, pu
V_0 slack bus voltage, pu
VCC_k variable capital cost of continuous technology k, $/kW
$X_{n,n'}$ inductance of line (n,n′), pu

Decision variables

$\Delta Pb_{n,s,t}$ output power increase from battery, kW
$\Delta Pg_{n,g,t}^{LstPrt}$ contribution of the partial load unit from discrete technology g at bus n to the post-contingency dispatch, kW
$\Delta Pg_{n,g,t}^{Min}$ output power increase from minimum load units, kW
$\Delta Pg_{n,g,t}^{Prt}$ output power increase from partial load unit, kW
$bi_{n,k}$ binary investment decision for technology k at node n
$bp_{n,g,t}$ binary variable for the existence of a partial load unit
$bx_{n,g,t}$ binary variable for the existence of a maximum load unit
$ni_{n,g}$ integer number of installed units from discrete generation technology g at node n
$nm_{n,g,t}$ integer number of minimum load units from discrete technology g
$no_{n,g,t}$ integer number of operating units from discrete technology g at node n at time t
$nx_{n,g}$ integer number of maximum load units from discrete technology g
$C_{n,k}$ capacity of continuous technology k at node n, kW for generation or kWh for storage technologies
$CR_{n,s,t}$ charge rate (input power) of storage technology s at node n at time t, kW
$DR_{n,s,t}$ discharge rate (output power) of storage technology s at node n at time t, kW
$E_{n,s,t}$ energy stored (state of charge) in storage technology s at node n at time t, kWh
$H_{n,n',t}$ heat flow from node n to n′ at time t, kW
$P_{n,n',t}$ active power flow in line (n,n′) at time t, per unit
$Pg_{n,j,t}$ generation of technology j at node n, kW
$Pg_{n,g,t}^{Lst}$ largest generation among all of the units from technology g at bus n at time t, kW
$Pg_{n,g,t}^{Prt}$ generation of the partial load unit from technology g at node n at time t, kW
$Pi_{n,t}$ injected active power at node n, pu
$Pl_{n,t}^{Cur}$ electrical load not met at node n following a contingency at time t, kW
$Q_{n,n',t}$ reactive power flow in line (n,n′) at time t, per unit
$Qi_{n,t}$ injected reactive power at node n, pu
$VS_{n,t}$ voltage magnitude squared at node n, pu

II. Introduction

THE attention towards microgrids is increasing at a fast pace, due to their benefits in terms of renewable integration, low carbon footprint, reliability and resiliency, power quality, and economics. However, microgrids have been the only solution for rural and off-grid communities for a long time, due to the limited/lack-of access to the main grid [1]. Traditionally, these off-grid communities relied on diesel generation to supply their loads, despite the higher fuel prices in the remote areas, but nowadays with increased global environmental concerns and incentives for a transformation of these diesel-based systems into renewable-based microgrids, changes can be observed [2]. This transition to resources with high variability and uncertainty, such as wind and photovoltaic, requires new microgrid planning tools to ensure the security of supply of these isolated systems.

A comprehensive microgrid investment and planning optimization must address (a) power generation mix selection; (b) resource sizing and allocation; (c) operation scheduling [3]; and (d) interplay between electricity, cooling, and heating loops in the microgrid to take full advantage of excess heat. (e) Moreover, in the context of remote/isolated microgrids, accounting for security of supply constraints in the design and operation is needed. A review of the literature (comprehensive reviews of many of the existing tools and computer models for renewable energy integration and microgrid planning can be found in [3]–[5]) shows that most of the existing models focus on individual sub-problems and do not include the others, or include them without enough depth.

Several examples of microgrid design formulations that only tackle the electrical energy flow, neglecting heating and cooling, are given in [6]–[9]. Among this category are also some of the distribution network planning formulations [10]–[13] that consider distributed energy resources (DER), since they share some of the same characteristics with the microgrid design problem. These methods only model electrical energy use and usually consider a limited generation mix.

Among the models that account for different energy uses are [14]–[18]. Omu et al. [14] formulated a mixed integer linear program for the technology selection, unit sizing, unit allocation, and distribution network structure of a distributed energy system that meets the electricity and heating demands of a cluster of buildings. This work, however, models electrical energy as a commodity whose transfer from one location to another is decided without physical laws, i.e. power flow constraints or Kirchhoff laws. Similarly, [15]–[17] present approaches for design and planning of urban and distributed energy systems, but do not include power flow equations. Basu et al. use power loss sensitivity to guide the optimization in

siting Combined Heat and Power (CHP)-based DERs in [18]. Although both electrical and thermal networks are modeled, the formulation is nonlinear, and solves using a stochastic approach, which entails a significant computational burden. Furthermore, obtaining an optimal solution is not scalable in such solution methods.

The existing literature also includes references that consider security of supply in the microgrid design. In the literature on grid-connected systems, some methods focus on improving the reliability and security of supply in the distribution system, through leveraging the design of multiple distribution system connected microgrids [19]–[21]. Alternatively, in the context of an individual microgrid, some references integrate security of supply indices, e.g. Loss of Load Expectation (LOLE), as constraints into the problem of optimal sizing and placement of DERs in the microgrid. However, due to the probabilistic nature of the indices, these methods result in nonlinear stochastic formulations [22] that require complex solution methodologies, e.g., meta-heuristics combined with Monte Carlo simulations [23] or Robust Optimization combined with Benders decomposition [7]. Although these methods can capture the uncertainty associated with the security of supply, they cannot be applied to complex multi-energy microgrids due to two main reasons: First, they mostly fail to capture the interplay between electricity, heating, and cooling loads and sources. Second, these techniques entail significant computational burdens and cannot guarantee a certain degree of optimality, especially when applied to large problems such as multi-energy microgrids.

To address the gap in the literature, this paper aims at including the security of supply constraint in the optimal design of isolated multi-energy microgrids and proposes a novel model for N-1 security-constrained design of such systems. The proposed model builds on the Distributed Energy Resources Customer Adoption Model (DER-CAM) developed by Lawrence Berkeley National Laboratory [24], [25]. The contributions of this work are threefold:

- First, we propose an integrated design approach that determines the optimal mix, size, location, and dispatch of renewable and fossil fuel-based DERs in multi-energy microgrids with electricity, heating, and cooling energy uses. To meet the electrical and thermal network constraints, we integrate linear power flow (*LinDistFlow*) and heat transfer equations into this formulation.
- Second, we integrate a set of linear constraints into the optimization problem that ensure security of supply against N-1 generator contingencies. The constraints are developed such that the optimization run time remains tractable.
- And third, we apply the proposed formulation to an example isolated microgrid developed based on a real isolated microgrid in Alaska.

This paper is organized as follows. Section III introduces the mathematical model for integrated design of multi-energy microgrids, i.e. a microgrid with electrical, heating, and cooling loads, which includes cabling (electrical) and piping (heating) networks. Section IV presents our proposed model for the security-constrained design and operation of the microgrid. In section V, the example case of an isolated utility microgrid in Alaska is studied and discussed. Finally, conclusions and future work are presented in section VI.

III. Mathematical Model for Integrated Design of Multi-Energy Microgrids

The goal is to develop a model that determines the optimal mix, capacity, and siting (placement) of various DER technologies that minimize (a) the overall investment and operation cost and/or (b) the overall CO_2 emissions, while ensuring security of the supply. Since the optimization model becomes very large and due to the superiority of Mixed Integer Linear Program (MILP) solvers over nonlinear ones, we formulate the problem as a MILP, by making necessary simplifying assumptions, to keep the problem solvable in reasonable and practical run times.

We consider a generic microgrid structure that has a radial electrical network and an arbitrary piping network. The load at each node is composed of electricity (plug loads), heating (space- and water-heating), and cooling (space-cooling and refrigeration) end-uses. Recognizing these three end-uses enables the formulation to optimally meet the loads by leveraging the synergies between different energy carriers, since each end-use can be met by multiple technologies. For instance:

- a combination of conventional generators, renewable resources, and battery technologies can be used to supply electrical end-uses;
- cooling loads can be met by electrical chillers, absorption chillers, or cold storage technoliges; and
- heating loads can be met by gas-fired boilers, recovered heat from CHP technologies, and heat storage technologies.

A visual representation of our energy conversion model is depicted in Fig. 1 (similar examples can be found in [26], [27]), showing sources and sinks of electricity, heating, and cooling, at each of the microgrid nodes. In this figure, different forms of energy are shown with different arrow heads to enhance readability and also emphasize on the energy conversion. For instance, waste heat from CHP technologies (e.g., ICE, MT, or FC) is recovered by heat exchangers (HX). Other examples are conversion of electrical and heating into cooling by electric (EC) and absorption chillers (AC), respectively.

A. Continuous vs. discrete investment decision variables

We model capacity of DER technologies using a continuous or discrete variable: If a technology is available in small enough modules (e.g. photovoltaic and storage), the optimal capacity is modeled as a continuous variable, significantly lowering the computation time. These technologies are referred to as *continuous* technologies. Discrete variables are used otherwise (e.g. micro-turbines) and called *discrete* technologies. Whenever possible, we use continuous variables to model the installed capacity of a given technology, as this significantly contributes to reducing the model runtime.

B. Time resolution

We propose to use typical day-types to model a full year. More specifically, we define a typical “week” day, “weekend” day, and “peak” (e.g. outlier in terms of larger load or larger ramp rate) day per month, where each one is modeled with

representative hourly load profiles. As a result, our proposed formulation models a year with 12×3×24 time-steps, which is less than one-tenth of the number of time-steps in the more common 8,760-hour modeling. This gain is obtained without losing any valuable information in the load profiles, since the impact of peak days on component sizing is captured through inclusion of "peak" days; and the operation cost is mostly determined by typical "week" and "weekend" day-types due to their higher frequency of occurrence. It is worth noting that the formulation can be generalized to include multiple "peak" day types, e.g., one "peak" day profile per end-use or energy carrier.

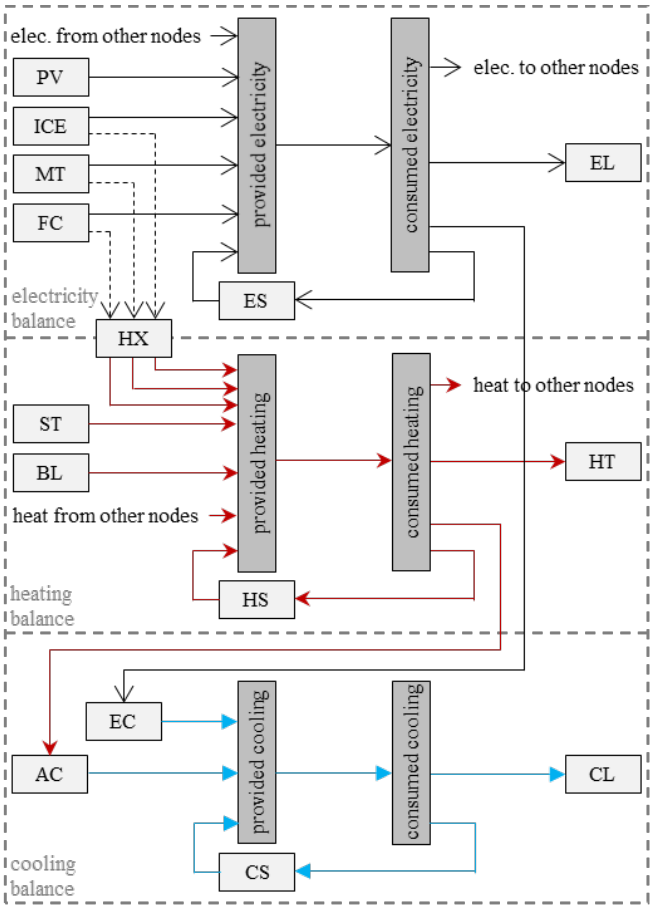

Fig. 1. Energy conversion and balance at each microgrid node

C. MILP optimization model

The objective is to minimize the overall microgrid investment and operation cost (1) or its CO_2 emissions (2), or a combination of the two objectives. The overall cost (1) includes annualized investment costs of technologies, where annuity rate depends on the interest rate and technology lifetime; generation cost for electrical, heating, or cooling technologies; and cost of post-contingency load curtailments. The emission objective (2) captures CO_2 emissions from the operation of all technologies.

$$\begin{aligned} C^{\text{Cost}} &= \sum_{\text{n,g}} ni_{\text{n,g}} \cdot \overline{\text{P}}_{\text{g}} \cdot \text{TCC}_{\text{g}} \cdot \text{AR}_{\text{g}} \\ &+ \sum_{\text{n,k}} \left(\text{FCC}_{\text{k}} \cdot bi_{\text{n,k}} + \text{VCC}_{\text{k}} \cdot C_{\text{n,k}}\right) \cdot \text{AR}_{\text{k}} \\ &+ \sum_{\text{n,j,t}} Pg_{\text{n,j,t}} \cdot \text{GC}_{\text{j}} \\ &+ \sum_{\text{n,t}} Pl^{\text{Cur}}_{\text{n,t}} \cdot \text{CC}_{\text{n}} \end{aligned} \tag{1}$$

$$C^{\text{CO2}} = \sum_{\text{n,j,t}} Pg_{\text{n,j,t}} \cdot \text{CER}_{\text{j}} \tag{2}$$

It is worth noting that the operation costs in (1) are scaled up from the 864 time-steps to 8,760 time-steps by considering the number of day-types per month, e.g., 20 "week" days, 8 "weekend" days, and 2 "peak" days. the scaling is now shown in (1) to simplify the presentation of the equation.

We adopted *LinDistFlow,* a distribution-level tractable linear balanced AC power flow model [28], [29]. This model (3)-(6) is advantageous over the well-known DC power flow approximation, since it allows for voltage magnitude deviations in the network, considers line resistances, and models both active and reactive power flow in the network. The net injected active power at a node, $Pi_{\text{n,t}}$, accounts for DER generation, electric load, electric chiller consumption, and electric storage system charging/discharging (7). Equations (8)-(9) enforce bus voltage constraints and line power constraints in the network, respectively. To linearize line power capacity constraints, we use an inner approximation of the exact constraint, i.e. the octagon in Fig. 2. instead of the circle, using the constraints in (9).

$$VS_{\text{n,t}} - VS_{\text{n}',\text{t}} = 2 \cdot \left(\text{R}_{\text{n,n}'} \cdot P_{\text{n,n}',\text{t}} + \text{X}_{\text{n,n}'} \cdot Q_{\text{n,n}',\text{t}}\right) \tag{3}$$

$$VS_{\text{n=1,t}} = \text{V}_0^2 \tag{4}$$

$$Pi_{\text{n,t}} = \sum_{\text{n}'} P_{\text{n,n}',\text{t}} \tag{5}$$

$$Qi_{\text{n,t}} = \sum_{\text{n}'} Q_{\text{n,n}',\text{t}} \tag{6}$$

$$\begin{aligned} \text{Sb} \cdot Pi_{\text{n,t}} &= \sum_{\text{j}\in\{\text{PV,ICE,MT,FC}\}} Pg_{\text{n,j,t}} - \text{Pl}_{\text{n,u=EL,t}} \\ &- \frac{1}{\text{CP}^{\text{e}}} \cdot Pg_{\text{n,c=EC,t}} \\ &+ DR_{\text{n,s=ES,t}} \cdot \eta^{\text{D}}_{\text{s=ES}} - \frac{1}{\eta^{\text{C}}_{\text{s=ES}}} \cdot CR_{\text{n,S=ES,t}} \end{aligned} \tag{7}$$

$$\underline{\text{V}}^2 \le VS_{\text{n,t}} \le \overline{\text{V}}^2 \tag{8}$$

$$\begin{aligned} \pm Q_{\text{n,n}',\text{t}} \le \text{cotan}\left(\left(\frac{1}{2} - \text{e}\right)\frac{\pi}{4}\right) \cdot \left(P_{\text{n,n}',\text{t}} - \cos\left(\text{e}\frac{\pi}{4}\right) \cdot \overline{\text{S}}_{\text{n,n}'}\right) \\ + \sin\left(\text{e}\frac{\pi}{4}\right) \cdot \overline{\text{S}}_{\text{n,n}'} \qquad \text{e} \in \{1, \dots, 4\} \end{aligned} \tag{9}$$

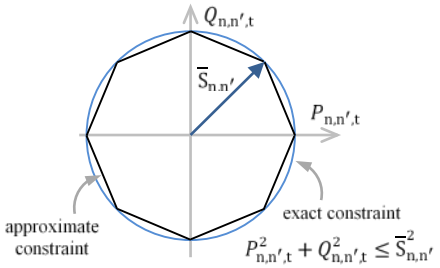

Fig. 2. Approximation of line capacity constraints

The heat balance equation at each node (10) accounts for heat generation; recovered CHP heat; heating loads inclusive of the required heat for absorption chilling, heat from/to storage technologies; and heat transfer between nodes through the piping network considering losses. Equation (11) enforces the pipe capacities. The cooling load at each node can be met by a combination of electric and absorption chilling and energy from cold storage technology (12).

$$\begin{aligned} 0 \quad = & \sum_{j\in\{ST,BL\}} Pg_{n,j,t} + \sum_{g\in\{ICE,MT\}} \alpha_g \cdot Pg_{n,g,t} \\ & - \mathrm{Pl}_{n,u=HT,t} - \frac{1}{\mathrm{CP}^a} \cdot Pg_{n,j=AC,t} \\ & - \frac{1}{\eta^C_{s=HS}} \cdot CR_{n,s=HS,t} + \eta^D_{s=HS} \cdot DR_{n,s=HS,t} \\ & - \sum_{n'} H_{n,n',t} + \sum_{n'} (1-\gamma_{n,n'}) \cdot H_{n',n,t} \end{aligned} \tag{10}$$

$$0 \le H_{n,n',t} \le \overline{H}_{n,n'} \tag{11}$$

$$\begin{aligned} 0 \quad = & \sum_{c\in\{AC,EC\}} Pg_{n,c,t} - \mathrm{Pl}_{n,u=CL,t} \\ & + \eta^D_{s=CS} \cdot DR_{n,s=CS,t} - \frac{1}{\eta^C_{s=CS}} \cdot CR_{n,s=CS,t} \end{aligned} \tag{12}$$

The literature on district heating networks includes a wide spectrum of modeling approaches, ranging from simple linear models with linear heat loss equations [17] to complex nonlinear models that include details such as network heat and pressure loss, temperature dynamics, etc. [30]. In this work, we use the former approach, in order to preserve optimization model linearity.

The energy (E) in electrical, heat, and cold storage technologies, considering self-discharge, are tracked (13) and kept within limits (14). The rate of charging (CR) and discharging (DR) is also limited (15).

$$E_{n,s,t} = (1-\varphi_s) \cdot E_{n,s,t-1} + CR_{n,s,t} \cdot \Delta t - DR_{n,s,t} \cdot \Delta t \tag{13}$$

$$\underline{E}_s \le E_{n,s,t} \le \overline{E}_s \tag{14}$$

$$CR_{n,s,t} \le C_{n,s} \cdot \overline{CR}_s, \quad DR_{n,s,t} \le C_{n,s} \cdot \overline{DR}_s \tag{15}$$

It is worth noting while a heat storage can be charged and discharged simultaneously (through different cycles), an electrical storage cannot. Therefore, it is common to use binary operational variables for an electrical storage unit to prevent simultaneous charging and discharging, e.g. [25]. However, since we consider non-ideal charging and discharging efficiencies (efficiency less than 100%), the model does not need to include such binary variables, as the optimization inherently picks a charging/discharging mode at each step and avoids simultaneous charging/discharging, in order to minimize the cost associated with charging/discharging loss. Our approach results in the same solution (given the optimization is solved with a good accuracy), while using fewer decision variables and constraints. More specifically, the proposed approach saves one binary decision variable and one constraint per node per time-step.

The dispatch of each technology does not exceed its maximum capacity and/or potential, or fall below the minimum acceptable limit (16)-(19).

$$Pg_{n,c,t} \le C_{n,c} \cdot \mathrm{SP}_t; \quad c \in \{\mathrm{PV}, \mathrm{ST}\} \tag{16}$$

$$no_{n,g,t} \cdot \underline{P}_g \le Pg_{n,g,t} \le no_{n,g,t} \cdot \overline{P}_g \tag{17}$$

$$no_{n,g,t} \le ni_{n,g} \tag{18}$$

$$Pg_{n,c,t} \le C_{n,k} \le bi_{n,k} \cdot M \tag{19}$$

To ensure economic feasibility of the microgrid design, more constraints may be integrated into the model, in which: a) saving in the operational cost of the microgrid is calculated against a base-case (i.e., business-as-usual case); and b) an investment payback constraint is defined that takes into account investment cost, operational cost saving, interest rate, and lifetime of various technologies. Detailed discussion of payback constraints can be found in [25].

IV. Mathematical Model for Security Constraints

In our proposed security-constrained design approach, a series of constraints are integrated into the optimization to ensure the system has enough reserve generation online to make up for the loss of any single generation or storage unit, considering ramping constraints. It is assumed that thermal loads in the system are not critical and the system can tolerate their curtailment. Consequently, only electrical contingencies are taken into account, and thermal generation and storage outages are not considered. Furthermore, following an electrical contingency, the microgrid must supply electrical end-use loads, and thermal end-use loads may be curtailed without a penalty.

As shown in Fig. 3, when an outage happens, the remaining generators (and storage devices) are given some time (Δt^{ctgrmp}) to ramp up. After this period, the total system generation must be enough to meet the loads (considering any load curtailment).

We model outage of continuous and discrete technologies differently, as depicted in Fig. 4:

- When considering a continuous technology (e.g. photovoltaic) outage at a node, its entire generation ($Pg_{n,c,t}$) at the node will be lost. That is because it is assumed that the entire capacity ($C_{n,c}$) is installed in one unit.
- In contrast, since we allow for several units from a discrete technology ($ni_{n,g}$) to be installed at a node, only a portion (generation of a single unit) of the aggregate generation ($Pg_{n,g,t}$) is lost in an outage. Therefore, although only the aggregate generation of a technology at a node ($Pg_{n,g,t}$) is relevant for power flow modeling, knowledge about generation of individual units is needed for contingency analysis.

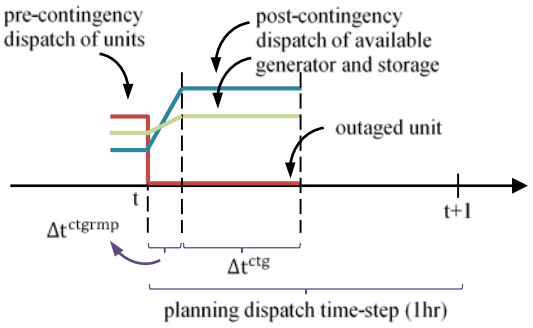

Fig. 3. Timing assumptions for the contingency analysis

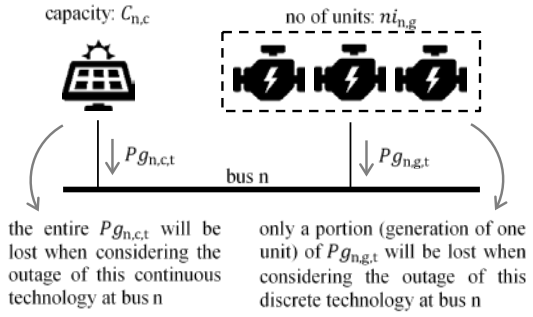

Fig. 4. Lost generation power for continuous and discrete technology outages

It is common practice in security-constrained dispatch formulations [31], [32] to track the generation of individual generator units. In our design formulation, this practice will translate into disaggregating the generation of a group of units from a technology ($Pg_{n,g,t}$) into the maximum number of units that can be installed from a technology at a bus, e.g. 10 units, and tracking the generation of each unit in order to formulate N-1 contingency constraints. This approach, however, will impose a significant computation burden on the solver, since it entails a large number of continuous and binary decision variables and constraints. Note that in order to impose the minimum generation limit on each unit, a binary decision variable is required to track the online/offline status of each unit at each time-step.

To address this challenge and integrate N-1 security constraints efficiently with fewer decision variables, we propose a novel approach, where the units from each discrete technology type (at a node) are classified into three categories and the aggregated generation of each category is tracked, instead of the generation of each unit. The three categories are:

- the units operating at the minimum load;
- the units operating at the maximum load; and
- the unit operating at partial load, i.e. between minimum and maximum loads (note: no more than one unit).

This classification of the units is due to the tradeoff between operating efficiency and reserve capacity: On one hand, the optimal dispatch tends to run a generator unit at its maximum load ($\overline{P}_g$) due to higher efficiency. On the other hand, consideration of generator outages motivates the optimization to run more units at their minimum load ($\underline{P}_g$), in order to increase the reserve in the system. Therefore, the proposed categories capture the tradeoffs between running the units at maximum load vs. minimum load. The consideration of one partial load unit is to enable disaggregation of any arbitrary value of $Pg_{n,g,t}$ into the three categories.

Equations (20)-(22) show how we disaggregate $Pg_{n,g,t}$ and $no_{n,g,t}$ into the number of units operating at the minimum load ($nm_{n,g,t}$), number of units operating at the maximum load ($nx_{n,g,t}$), and generation power of the unit operating at a partial load ($Pg^{Prt}_{n,g,t}$). Binary variable $bp_{n,g,t}$ denotes whether a partial load unit exists. To simplify the contingency constraints, it is assumed that a partial load unit always exists ($bp_{n,g,t} = 1$) if $no_{n,g,t} > 0$ (23).

$$no_{n,g,t} = nm_{n,g,t} + nx_{n,g,t} + bp_{n,g,t} \tag{20}$$

$$Pg_{n,g,t} = Pg^{Prt}_{n,g,t} + nm_{n,g,t} \cdot \underline{P}_g + nx_{n,g,t} \cdot \overline{P}_g \tag{21}$$

$$bp_{n,g,t} \cdot \underline{P}_g \le Pg^{Prt}_{n,g,t} \le bp_{n,g,t} \cdot \overline{P}_g \tag{22}$$

$$bp_{n,g,t} \cdot M \ge no_{n,g,t} \tag{23}$$

Next, we develop equations that determine the maximum possible contribution of each DER to the post-contingency state of the system. The maximum output change for minimum load units after a contingency happens, $\Delta Pg^{Min}_{n,g,t}$, is limited by the unused capacity of the units (24) and their maximum rate of change (25). Similarly, the maximum contribution of a partial load unit, $\Delta Pg^{Prt}_{n,g,t}$, is limited by its unused capacity (26) and the maximum rate of change (27). Maximum load units cannot increase their generations if a contingency happens.

The output change for an electric storage system is limited by its maximum ramp rate (28). Also, since the post-contingency dispatch must be sustainable for a period of Δt^{ctg} (see Fig. 3), storage system must be able to keep its post-contingency output for this period (29). Since renewable generation technologies are assumed to be operating at their maximum potential at all times, these units cannot increase their generation in the post-contingency state.

$$\Delta Pg^{Min}_{n,g,t} \le \left(\overline{P}_g - \underline{P}_g\right) \cdot nm_{n,g,t} \tag{24}$$

$$\Delta Pg^{Min}_{n,g,t} \le \overline{PgR}_g \cdot \overline{P}_g \cdot \Delta t^{ctgrmp} \cdot nm_{n,g,t} \tag{25}$$

$$\Delta Pg^{Prt}_{n,g,t} \le \overline{P}_g - Pg^{Prt}_{n,g,t} \tag{26}$$

$$\Delta Pg^{Prt}_{n,g,t} \le \overline{PgR}_g \cdot \overline{P}_g \cdot \Delta t^{ctgrmp} \cdot bp_{n,g,t} \tag{27}$$

$$\Delta Pb_{n,s=ES,t} \le \overline{DR}_{s=ES} \cdot C_{n,s=ES} - DR_{n,s=ES,t} \tag{28}$$

$$\Delta t^{ctg} \cdot \left(\Delta Pb_{n,s=ES,t} + DR_{n,s=ES,t}\right) \le E_{n,s=ES,t} \tag{29}$$

To integrate reserve equations into the security-constrained optimal dispatch, the traditional approach [31], [33] is to impose a fixed (static) reserve requirement, such as size of the largest system generator or a percentage of total system load. However, dynamic allocation of system reserve [34], [35] can offer a less conservative and more economical solution. To this end, we develop a novel set of reserve equations that dynamically allocate reserve in the system depending on the generation of different technologies, storage system state of charge, technology ramping constraints, etc. The dynamic reserve equations (security constraints) against outage of renewable (continuous) generation technologies, storage

technologies, and conventional (discrete) generation technologies are presented in (30)-(32), respectively. For each outage, the pre-contingency generation power of the outaged unit must be less than the available reserve in the system, where the available reserve is composed of:

- generation increase in discrete technologies (minimum load units and partial load unit);
- increase in storage output; and
- post-contingency load curtailment including electric chiller load and storage charging load (since they will not be met during the contingency period).

The reserve capacity in the system must be larger than the generation of each continuous unit at each bus n at any given time t (30), where all of the system discrete generators and batteries can contribute to the system reserve. Furthermore, post-contingency electrical load curtailments ($Pl^{\mathrm{Cur}}_{\mathrm{n}',\mathrm{t}}$), as well as pre-contingency storage charging and electric chiller loads that will be shed, can be leveraged to increase the system reserve. Equation (31) imposes a similar constraint considering the outage of the storage system at any bus n. Note that all of the system batteries, except for the battery whose outage is being constrained (hence the negative term in the reserve calculation), can contribute to the reserve.

$$\begin{aligned} Pg_{\mathrm{n,c=PV,t}} \leq & \sum_{\mathrm{n}',\mathrm{g},\mathrm{t}} \left(\Delta Pg^{\mathrm{Min}}_{\mathrm{n}',\mathrm{g},\mathrm{t}} + \Delta Pg^{\mathrm{Prt}}_{\mathrm{n}',\mathrm{g},\mathrm{t}}\right) \\ & + \sum_{\mathrm{n}'} \Delta Pb_{\mathrm{n}',\mathrm{s=ES},\mathrm{t}} \\ & + \sum_{\mathrm{n}'} Pl^{\mathrm{Cur}}_{\mathrm{n}',\mathrm{t}} \\ & + \sum_{\mathrm{n}'} CR_{\mathrm{n}',\mathrm{s=ES},\mathrm{t}} + \sum_{\mathrm{n}'} \frac{1}{\mathrm{CP^e}} \cdot Pg_{\mathrm{n}',\mathrm{c=EC},\mathrm{t}} \end{aligned} \tag{30}$$

$$\begin{aligned} DR_{\mathrm{n,s=ES,t}} \leq & \sum_{\mathrm{n}',\mathrm{g},\mathrm{t}} \left(\Delta Pg^{\mathrm{Min}}_{\mathrm{n}',\mathrm{g},\mathrm{t}} + \Delta Pg^{\mathrm{Prt}}_{\mathrm{n}',\mathrm{g},\mathrm{t}}\right) \\ & + \sum_{\mathrm{n}'} \Delta Pb_{\mathrm{n}',\mathrm{s=ES},\mathrm{t}} - \Delta Pb_{\mathrm{n,s=ES},\mathrm{t}} \\ & + \sum_{\mathrm{n}'} Pl^{\mathrm{Cur}}_{\mathrm{n}',\mathrm{t}} \\ & + \sum_{\mathrm{n}'} CR_{\mathrm{n}',\mathrm{s=ES},\mathrm{t}} + \sum_{\mathrm{n}'} \frac{1}{\mathrm{CP^e}} \cdot Pg_{\mathrm{n}',\mathrm{c=EC},\mathrm{t}} \end{aligned} \tag{31}$$

$$\begin{aligned} Pg^{\mathrm{Lst}}_{\mathrm{n,g,t}} \leq & \sum_{\mathrm{n}',\mathrm{g}',\mathrm{t}} \left(Pg^{\mathrm{Min}}_{\mathrm{n}',\mathrm{g}',\mathrm{t}} + \Delta Pg^{\mathrm{Prt}}_{\mathrm{n}',\mathrm{g}',\mathrm{t}}\right) \\ & - \Delta Pg^{\mathrm{PrtLst}}_{\mathrm{n,g,t}} \\ & + \sum_{\mathrm{n}'} \Delta Pb_{\mathrm{n}',\mathrm{s=ES},\mathrm{t}} \\ & + \sum_{\mathrm{n}'} Pl^{\mathrm{Cur}}_{\mathrm{n}',\mathrm{t}} \\ & + \sum_{\mathrm{n}'} CR_{\mathrm{n}',\mathrm{s=ES},\mathrm{t}} + \sum_{\mathrm{n}'} \frac{1}{\mathrm{CP^e}} \cdot Pg_{\mathrm{n}',\mathrm{c=EC},\mathrm{t}} \end{aligned} \tag{32}$$

In (32) for imposing the security constraint for discrete generator outages, $Pg^{\mathrm{Lst}}_{\mathrm{n,g,t}}$ is the largest generation power among all of the units from technology g connected to bus n. Hence, $Pg^{\mathrm{Lst}}_{\mathrm{n,g,t}}$ is $\overline{\mathrm{P}}_{\mathrm{g}}$ if there is a unit operating at maximum load (33)-(34), or otherwise, is the power of the partial load unit (35). The variable $\Delta Pg^{\mathrm{PrtLst}}_{\mathrm{n,g,t}}$ is used to negate the contribution of the outaged unit from the total contribution of the units. It is 0 if the outaged unit is a maximum load unit (when $bx_{\mathrm{n,g,t}}$, a binary variable that denotes whether a maximum load unit exists, is one) and is $\Delta Pg^{\mathrm{Prt}}{}_{\mathrm{n,g,t}}$ if the outaged unit is a partial load unit (when $bx_{\mathrm{n,g,t}} = 0$), as shown in (36).

$$Pg^{\mathrm{Lst}}_{\mathrm{n,g,t}} \geq bx_{\mathrm{n,g,t}} \cdot \overline{\mathrm{P}}_{\mathrm{g}} \tag{33}$$

$$bx_{\mathrm{n,g,t}} \leq nx_{\mathrm{n,g,t}} \leq bx_{\mathrm{n,g,t}} \cdot \mathrm{M} \tag{34}$$

$$Pg^{\mathrm{Lst}}_{\mathrm{n,g,t}} \geq Pg^{\mathrm{Prt}}_{\mathrm{n,g,t}} \tag{35}$$

$$\Delta Pg^{\mathrm{PrtLst}}_{\mathrm{n,g,t}} \geq \Delta Pg^{\mathrm{Prt}}_{\mathrm{n,g,t}} - bx_{\mathrm{n,g,t}} \cdot \overline{\mathrm{P}}_{\mathrm{g}} \tag{36}$$

V. Case Study

A. Case setup

We developed an isolated microgrid test system based on a real-life remote utility microgrid in Nome, Alaska [36]. This model is composed of 19 nodes and its GIS and electrical and thermal single line diagrams are shown in Fig. 5. The important technology parameters are shown in Table I and Table II. More details can be provided upon request.

We consider three cases. In *Case I* the objective is to minimize overall costs, but N-1 contingency constraints are not included. In *Case II*, we minimize the overall costs while including the contingency constraints. In *Case III*, a composite objective (50% weight for cost objective and 50% weight for CO_2 emission objective) is considered and security constraints are also taken into account. In each case, the optimization model determines the optimal mix and size of discrete (1,000 and 5,000 kVA CHP-enabled diesel engines) and continuous (photovoltaic, battery, boiler, and electric chiller) technologies that can be installed at nodes 1, 8, and 18, which are the microgrid's central power plant, a hospital, and a residential neighborhood toward the end of a long feeder, respectively.

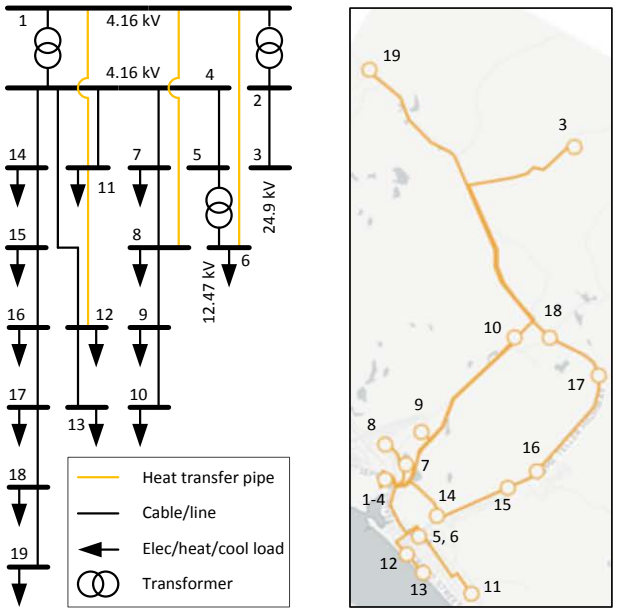

Fig. 5. Single line diagram and GIS view of the example isolated microgrid

TABLE I
INVESTMENT PARAMETERS FOR CONTINUOUS TECHNOLOGIES

Technology	Fixed Cost ($)	Variable Cost ($/kW)
Battery	75,000	500
Photovoltaic	40,000	4,000
Boiler	4,500	30
Electric Chiller	2,300	230

TABLE II
INVESTMENT AND OPERATION PARAMETERS FOR DISCRETE TECHNOLOGIES

Technology	Size (kW)	Cost ($/kW)	Eff. (%)	Min/Max Load (%)	Ramp Rt. (%/min)	Ht. Rec. Alpha
CHP Diesel	1,000	1,911	36.8%	30%, 100%	50%	1.019
CHP Diesel	5,000	1,182	41.6%	30%, 100%	50%	0.797

B. Optimal DER mix, capacity, and siting

The results of the case studies, including DER capacities at each node (i.e., n1, n8, and n18), annualized investment and annual operation costs, post-contingency load curtailment costs, and annual CO_2 emissions are summarized in Table III.

In Case I, only one unit of the 5,000 kVA CHP-enabled diesel generator is installed at the central power plant (node 1) without any photovoltaic or battery investments in the system. When the contingency constraints are added to the optimization model in Case II, a 2,833 kWh battery storage system is added to the optimal technology mix. Furthermore, the solution includes several small diesel units instead of one large unit (3×1,000 vs. 1×5,000 kVA), because several units operating in parallel enhance the system security against generator outage contingencies. Consequently, both investment and operation costs increase in Case II. It is worth noting that the optimal solution does not include any photovoltaic systems, mainly because they are not dispatchable and cannot contribute to the reserve constraints.

In Case III, cost minimization and emission reduction are considered with the same weight. Several observations can be made from the optimal investment solution. First, in order to reduce CO_2 emissions, 4,274 kW of photovoltaics are installed at note 8, although photovoltaic was not cost-effective in Case I and II. Second, the size of the battery storage system at node 8 becomes threefold larger compared to Case II. Third, compared to Case II, one of the 1,000 kVA diesel units at node 1 is replaced with a 5,000 kVA unit. The reason is that the larger unit has a higher efficiency (41.6% vs. 36.8%) and hence, can reduce CO_2 emissions. The optimal DER mix in Case III results in a 14% reduction in CO_2 emissions that is made possible by a 19% increase in the total annual investment and operation costs.

TABLE III
CASE STUDY RESULTS – OPTIMAL TECHNOLOGY MIX AND SITING

			Case I	Case II	Case III
DER Capacities	Photovoltaic (kw)	n1			
		n8			4,274
		n18			
	Battery (kWh)	n1			
		n8		2,883	8,220
		n18			
	CHP-enabled diesel engine (units × kVA cap)	n1	1×5,000	3×1,000	2×1,000 + 1×5,000
		n8			
		n18			
Costs	Operation (k$)		8,133	8,662	7,486
	Investment (k$)		962	1,240	4,291
	Curtailment (k$)		-	31	39
	Total (k$)		9,096	9,932	11,816
	CO_2 (tons)		16,104	16,650	14,329

C. Optimal electricity, heating, and cooling dispatch

To illustrate dispatch signals, Fig. 6 - Fig. 9 show optimal electrical and heating dispatch for multiple nodes in Case III. The optimal electrical dispatch for nodes 1 and 8 is shown in Fig. 6 and Fig. 7, respectively. Export of energy (to other nodes) is shown with negative values. The generation from the 3×1,000 kVA and 1×5,000 kVA diesel generators at node 1 is entirely exported to other nodes, since the node does not have any loads of its own. Node 8 is equipped with a photovoltaic and a battery system to supply its own load and export the extra power to other nodes. The battery is charged during peak photovoltaic hours and discharged at morning and afternoon. The interplay between electricity and cooling impacts the load in this figure, since it includes the electrical end-use loads as well as electrical consumption of chillers.

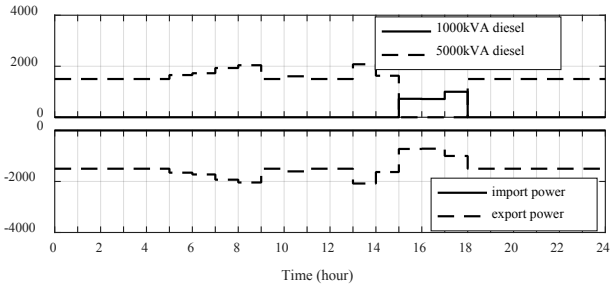

Fig. 6. Optimal electricity dispatch for node 1 (Case III, September weekday)

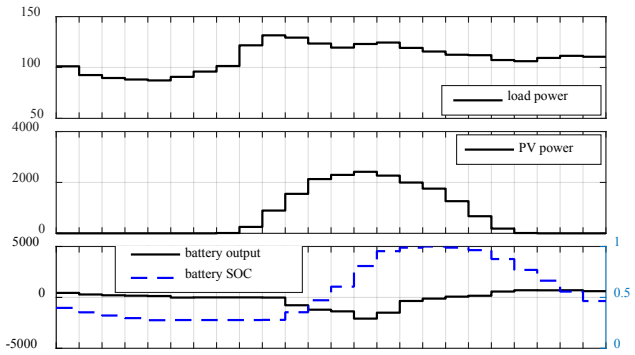

Fig. 7. Optimal electricity dispatch for node 8 (Case III, September weekday)

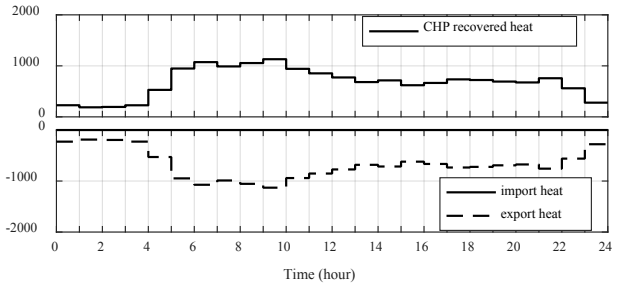

Fig. 8. Optimal heating dispatch for node 1 (Case III, July weekday)

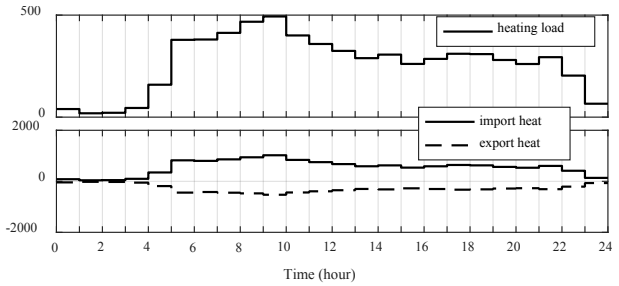

Fig. 9. Optimal heating dispatch for node 11 (Case III, July weekday)

The optimal heating dispatch for nodes 1 and 11 is shown in Fig. 8 and Fig. 9, respectively. The heat from diesel units at node 1 is recovered and exported to other nodes through pipes. The consideration of recovered heat ties the dispatch of electricity and heating in the system. The heating loads at node 11 are met by the heat imported to the node. This node also exports the extra heat (from import) to other microgrid nodes.

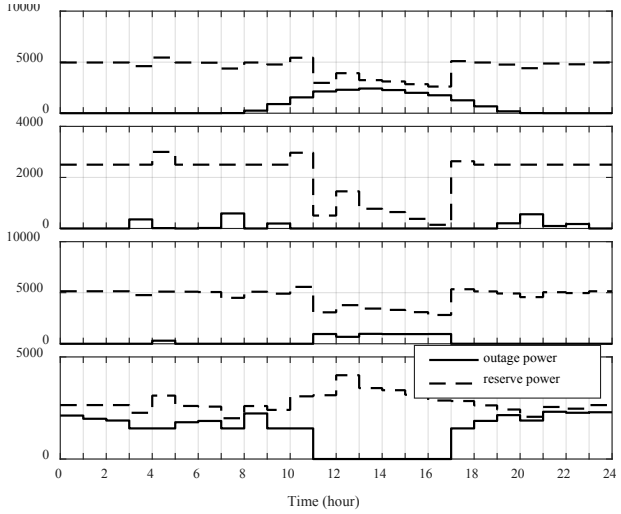

Fig. 10. Outage power vs. system reserve for various generator contingencies during a September peak day in Case III: (a) outage of the photovoltaic system at node 8; (b) outage of battery at node 8; (c) outage of one of the two 1,000 kVA diesel units at node 1; (d) outage of the 5,000 kVA diesel unit at node 1

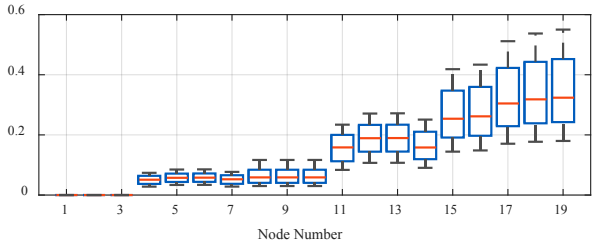

Fig. 11. Box plot for voltage magnitude error – Case III

D. Security against N-1 contingencies

Fig. 10 shows the generation outage power vs. system reserve for various generation contingencies during a September peak day in Case III (arbitrarily chosen), where the outage power and system reserve refer to the left-hand side and right-hand side terms in (30)-(32), respectively. As shown in this figure, the integration of security constraints forces the system reserve to be more than the outage power at any given time. In this example, outage of the 5,000 kVA diesel unit at node 1 is the most severe contingency, since it is much larger than all other dispatchable units in the system. Fig. 10(d) confirms this intuition and shows that although the system maintains enough reserve against this contingency, the difference between the outage power and the reserve in the system is much smaller compared to other contingencies.

E. Voltage profile and linear power flow accuracy

The box plot for voltage magnitude error at each microgrid node is shown in Fig. 11 for Case III, where the error is the % difference between the approximate voltage solution (from the optimization) and the exact voltage solution (obtained post-optimization using Newton-Raphson algorithm). The error increases as the node distance from the slack bus, i.e. node 1, increases. However, the maximum error is less than 0.6%, which shows a very high accuracy. Our analysis shows that in this case, >87% of voltage data points have an error less than 0.3% and >97% of data points have an error less than 0.5%.

VI. Conclusions and Future Work

This paper presents a novel approach for security-constrained optimal design of isolated multi-energy microgrids, formulated as a mixed integer linear program. Our optimal design entails optimal DER technology mix, size, and dispatch, and takes into account the interplay between electricity, heating, and cooling loads and sources in the system; and hence, is able to capture benefits of CHP technologies. To provide a secure design/operation against N-1 generator contingencies, a novel model was developed to dynamically assess the microgrid generation reserve.

To illustrate how the method works, several case studies were carried out on an isolated microgrid model that we developed based on a real isolated utility microgrid in Alaska and the impact of contingency constraints on the optimal solution was discussed. The studies showed that a cost-minimization design, especially in the presence of security constraints, may not lead to adoption of renewable resources, mainly due to their un-dispatchability and inability to ramp up generation following a system contingency. However, a cost-emission composite objective may lead to deployment of renewable technologies. Evaluating the accuracy of the integrated linear power flow equations (*LinDistFlow*) showed very high accuracy for the model.

Future research will focus on integrating network design (cable/pipe placement and sizing) into the model. We will also explore how renewable generation stochasticity can be incorporated into the optimization model. Furthermore, integration of non-electrical contingencies, e.g. outage of thermal resources, can also add to the value of this work.

VII. Acknowledgment

The authors gratefully thank Dan T. Ton, the Smart Grid R&D Program Manager at the US Department of Energy for his continuous support of the microgrid design tools at LBNL. We also thank the Nome Joint Utility Systems for providing data and operational insights for this work.

VIII. References

[1] T. Ackermann, *Wind power in power systems*. John Wiley & Sons, 2012.

[2] T. Simpkins, D. Cutler, B. Hirsch, D. Olis, and K. Anderson, "Cost-Optimal Pathways to 75% Fuel Reduction in Remote Alaskan Villages," pp. 125–130, 2015.

[3] C. Gamarra and J. M. Guerrero, "Computational optimization techniques applied to microgrids planning: A review," *Renew. Sustain. Energy Rev.*, vol. 48, no. 0, pp. 413–424, 2015.

[4] D. Connolly, H. Lund, B. V Mathiesen, and M. Leahy, "A review of computer tools for analysing the integration of renewable energy into various energy systems," *Appl. Energy*, vol. 87, no. 4, pp. 1059–1082, 2010.

[5] G. Mendes, C. Ioakimidis, and P. Ferrão, "On the planning and analysis of Integrated Community Energy Systems: A review and survey of available tools," *Renew. Sustain. Energy Rev.*, vol. 15, no. 9, pp. 4836–4854, 2011.

[6] J.-H. Teng, Y.-H. Liu, C.-Y. Chen, and C.-F. Chen, "Value-based distributed generator placements for service quality improvements," *Int. J. Electr. Power Energy Syst.*, vol. 29, no. 3, pp. 268–274, 2007.

[7] Z. Wang, B. Chen, J. Wang, J. Kim, and M. M. Begovic, "Robust optimization based optimal DG placement in microgrids," *IEEE Trans. Smart Grid*, vol. 5, no. 5, pp. 2173–2182, 2014.

[8] A. Khodaei and M. Shahidehpour, "Microgrid-based co-optimization of generation and transmission planning in power systems," *IEEE Trans. Power Syst.*, vol. 28, no. 2, pp. 1582–1590, 2013.

[9] M. V Kirthiga, S. A. Daniel, and S. Gurunathan, "A methodology for transforming an existing distribution network into a sustainable autonomous micro-grid," *IEEE Trans. Sustain. Energy*, vol. 4, no. 1, pp. 31–41, 2013.

[10] W. S. Tan, M. Y. Hassan, M. S. Majid, and H. Abdul Rahman, "Optimal distributed renewable generation planning: A review of different approaches," *Renew. Sustain. Energy Rev.*, vol. 18, pp. 626–645, 2013.

[11] B. Kroposki, P. K. Sen, and K. Malmedal, "Optimum sizing and placement of distributed and renewable energy sources in electric power distribution systems," *IEEE Trans. Ind. Appl.*, vol. 49, no. 6, pp. 2741–2752, 2013.

[12] D. D. Singh, D. D. Singh, and K. S. Verma, "Multiobjective optimization for DG planning with load models," *IEEE Trans. Power Syst.*, vol. 24, no. 1, pp. 427–436, 2009.

[13] C. L. T. Borges and D. M. Falcão, "Optimal distributed generation allocation for reliability, losses, and voltage improvement," *Int. J. Electr. Power Energy Syst.*, vol. 28, no. 6, pp. 413–420, 2006.

[14] A. Omu, R. Choudhary, and A. Boies, "Distributed energy resource system optimisation using mixed integer linear programming," *Energy Policy*, vol. 61, no. 0, pp. 249–266, 2013.

[15] J. Keirstead, N. Samsatli, N. Shah, and C. Weber, "The impact of CHP (combined heat and power) planning restrictions on the efficiency of urban energy systems," *Energy*, vol. 41, no. 1, pp. 93–103, 2012.

[16] E. D. Mehleri, H. Sarimveis, N. C. Markatos, and L. G. Papageorgiou, "Optimal design and operation of distributed energy systems: Application to Greek residential sector," *Renew. Energy*, vol. 51, no. 0, pp. 331–342, 2013.

[17] J. Söderman and F. Pettersson, "Structural and operational optimisation of distributed energy systems," *Appl. Therm. Eng.*, vol. 26, no. 13, pp. 1400–1408, 2006.

[18] A. K. Basu, A. Bhattacharya, S. Chowdhury, and S. P. Chowdhury, "Planned scheduling for economic power sharing in a CHP-based micro-grid," *IEEE Trans. Power Syst.*, vol. 27, no. 1, pp. 30–38, 2012.

[19] S. A. Arefifar, Y. A. R. I. Mohamed, and T. H. M. El-Fouly, "Supply-adequacy-based optimal construction of microgrids in smart distribution systems," *IEEE Trans. Smart Grid*, vol. 3, no. 3, pp. 1491–1502, 2012.

[20] S. A. Arefifar, Y. A. R. I. Mohamed, and T. H. M. El-Fouly, "Optimum microgrid design for enhancing reliability and supply-security," *IEEE Trans. Smart Grid*, vol. 4, no. 3, pp. 1567–1575, 2013.

[21] D. Jayaweera, "Security enhancement with nodal criticality-based integration of strategic micro grids," *IEEE Trans. Power Syst.*, vol. 30, no. 1, pp. 337–345, 2015.

[22] S. Bahramirad, W. Reder, and A. Khodaei, "Reliability-constrained optimal sizing of energy storage system in a microgrid," *IEEE Trans. Smart Grid*, vol. 3, no. 4, pp. 2056–2062, 2012.

[23] S. Abdi and K. Afshar, "Application of IPSO-Monte Carlo for optimal distributed generation allocation and sizing," *Int. J. Electr. Power Energy Syst.*, vol. 44, no. 1, pp. 786–797, 2013.

[24] S. Mashayekh, M. Stadler, G. Cardoso, and M. Heleno, "A mixed integer linear programming approach for optimal DER portfolio, sizing, and placement in multi-energy microgrids," *Appl. Energy*, vol. 187, pp. 154–168, Feb. 2017.

[25] T. Schittekatte, M. Stadler, G. Cardoso, S. Mashayekh, and N. Sankar, "The impact of short-term stochastic variability in solar irradiance on optimal microgrid design," *IEEE Transactions on Smart Grid*, vol. PP, no. 99. p. 1, 2016.

[26] X. Zhang, M. Shahidehpour, A. Alabdulwahab, and A. Abusorrah, "Optimal Expansion Planning of Energy Hub With Multiple Energy Infrastructures," *IEEE Transactions on Smart Grid*, vol. 6, no. 5. pp. 2302–2311, 2015.

[27] M. Stadler, M. Kloess, M. Groissböck, G. Cardoso, R. Sharma, M. C. Bozchalui, and C. Marnay, "Electric storage in California's commercial buildings," *Appl. Energy*, vol. 104, pp. 711–722, Apr. 2013.

[28] G. Lingwen and S. H. Low, "Convex relaxations and linear approximation for optimal power flow in multiphase radial networks," in *Power Systems Computation Conference*, 2014, pp. 1–9.

[29] M. E. Baran and F. F. Wu, "Optimal sizing of capacitors placed on a radial distribution system," *IEEE Trans. Power Deliv.*, vol. 4, no. 1, pp. 735–743, 1989.

[30] Z. Li, W. Wu, M. Shahidehpour, J. Wang, and B. Zhang, "Combined heat and power dispatch considering pipeline energy storage of district heating network," *IEEE Trans. Sustain. Energy*, vol. 7, no. 1, pp. 12–22, 2016.

[31] M. A. Fotouhi Ghazvini, H. Morais, and Z. Vale, "Coordination between mid-term maintenance outage decisions and short-term security-constrained scheduling in smart distribution systems," *Appl. Energy*, vol. 96, pp. 281–291, 2012.

[32] S. Mashayekh and K. L. Butler-Purry, "An integrated security-constrained model-based dynamic power management approach for isolated microgrids in all-electric ships," *IEEE Trans. Power Syst.*, vol. PP, no. 99, pp. 1–12, 2015.

[33] S. Y. Derakhshandeh, M. E. H. Golshan, and M. A. S. Masoum, "Profit-based unit commitment with security constraints and fair allocation of cost saving in industrial microgrids," *IET Sci. Meas. Technol.*, vol. 7, no. 6, pp. 315–325, 2013.

[34] L. E. Sokoler, P. Vinter, R. Baerentsen, K. Edlund, and J. B. Jorgensen, "Contingency-constrained unit commitment in meshed isolated power systems," *IEEE Trans. Power Syst.*, vol. 31, no. 5, pp. 3516–3526, 2016.

[35] J. F. Prada and M. D. Ilić, "Locational allocation and pricing of responsive contingency reserves," *IEEE Power Energy Soc. Gen. Meet.*, vol. 2015–Septe, 2015.

[36] "Alaska Energy Data Gateway." [Online]. Available: https://akenergygateway.alaska.edu/.

Lawrence Berkeley National Laboratory

One Cyclotron Road | Berkeley, California 94720

Prepared for the U.S. Department of Energy under Contract No. DE-AC02-05CH11231

15-PA-1015